Palladated cyclodextrin and halloysite containing polymer and its carbonized form as efficient hydrogenation catalysts

Samahe Sadjadi, Fatemeh Koohestani, Bastien Leger, Eric Monflier

Palladated cyclodextrin and halloysite containing polymer and its carbonized form as efficient hydrogenation catalysts

Samahe Sadjadi[1] | **Fatemeh Koohestani**[1] | **Bastien Léger**[2] | **Eric Monflier**[2]

[1]Gas Conversion Department, Faculty of Petrochemicals, Iran polymer and Petrochemicals Institute, PO Box 14975-112, Tehran, Iran

[2] Univ. Artois, CNRS, Centrale Lille, ENSCL, Univ. Lille, UMR 8181, Unité de Catalyse et de Chimie du Solide (UCCS), F-62300, Lens, France

Correspondence
Samahe Sadjadi, Gas Conversion Department, Faculty of Petrochemicals, Iran polymer and Petrochemicals Institute, PO Box 14975-112. Tehran, Iran.
Email: samahesadjadi@yahoo.com

Funding information
PHC GUNDISHAPUR 2018, Grant/Award Number: 40870ZG; Iran National Science Foundation, Grant/Award Number: 97009384; French Embassy; Center for International Scientific Studies & Collaborations (CISSC); European Regional Development Fund (ERDF); Conseil Régional du Nord-Pas de Calais

β-Cyclodextrin (β-CD) and glycidyl methacrylate monomer were polymerized in the presence of functionalized halloysite nanoclay (Hal) to afford a polymeric network (Hal-P-CD) containing Hal and CD. Hal-P-CD was then applied as a catalyst support for the immobilization of Pd nanoparticles. The resulting nanocomposite, Pd@Hal-P-CD, could serve as a catalyst for the hydrogenation of nitrobenzene. The precise study by the preparation of control samples confirmed the contribution of CD as both phase transfer and capping agent, P (polymer) and Hal to the catalysis. Moreover, the results confirmed the importance of CD: glycidyl methacrylate monomer ratio. Pd@Hal-P-CD was also carbonized to prepare Pd@Hal-C. Notably, the characterization of Pd@Hal-C showed that carbonization led to the growth of mean diameter of Pd nanoparticles, increase of Pd content and partial destruction of Hal. However, the catalytic activity of Pd@Hal-C was superior to Pd@Hal-P-CD. Pd@Hal-C was also highly recyclable and could be recovered and recycled for several reaction runs. The study of the carbonization temperature showed that this factor affected the nature of the resulting carbon and the catalyst prepared at elevated temperature showed higher catalytic activity.

KEYWORDS
carbonization, cyclodextrin, halloysite, heterogeneous catalyst, hydrogenation

1 | INTRODUCTION

In recent years, the use of halloysite nanoclay (Hal) as a catalyst support has gained growing interest and numerous heterogeneous Hal-based catalysts have been developed and successfully applied for promoting diverse organic transformations ranging from hydrogenation to coupling reactions.[1–7] Moreover, Hal has been utilized for the preparation of novel photocatalysts.[8–10] The excellent performance of Hal can be assigned to its distinguished physical and chemical properties, including biocompatibility, tubular morphology, opposite electrical charges and chemical composition on inner and outer surfaces and high mechanical resistance.[5–7,11,12] In attempt to improve the properties of Hal and broaden its applications, surface functionalization as well as formation of composite with other components such as polymers, dendrimers and carbon materials have been focused.[4,13,14]

β-cyclodextrin (CD) is a cyclic oligosaccharide composed of 7 glucose subunits with defined cone-shape structure, in which the exterior surface is hydrophilic, while the interior space is hydrophobic. The non-toxic, bio-compatible and relatively low cost of β-CD broaden its utility in various sectors such as food industry, design of delivery systems and catalysis.[15–17] The contribution of CD in the catalysis is mostly related to three main domains. First, CD can effectively act as a capping agent and prevent nano-catalysts from aggregations. More importantly, CD can host the hydrophobic substrates

inside its cavity and shuffle them to the hydrophilic media.[15–17] Beside, CD can be considered as an efficient precursor for the formation of carbon materials.[18–20]

Considering the wide range of use of aniline derivatives in the industrial sector, many attempts have been devoted to the development of efficient protocols for the synthesis of anilines through hydrogenation of nitrobenzenes.[21] This chemical process is mostly promoted in the presence of precious metals such as Pd. Taking the economic and environmental concerns into account, the use of heterogeneous precious metals has received increasing attention. Heterogenization can simply be achieved by immobilization of metallic species on the surface of an appropriate support or through encapsulation within the cavity of the porous support.[22–26]

In the continuation of our research on the development of efficient Hal-based heterogeneous catalysts,[27–29] recently, we have reported a novel catalyst with the utility for coupling reaction, in which Pd nanoparticles were immobilized on the composite of poly (glycidyl methacrylate) and Hal, in which Hal was covered with a shell of poly (glycidyl methacrylate).[30] The composite was simply synthesized through functionalization of Hal surface with 3-(trimethoxysilyl) propyl methacrylate followed by the polymerization with glycidyl methacrylate (M) monomer. The high catalytic activity of the catalyst motivated us to pursue our investigation on pol (glycidyl methacrylate)- Hal composite and develop a new catalyst based on that. On the other hand, our experiences showed that combination of chemistry of CD and Hal could increase the catalytic activity of the resulting catalyst due to the role of CD as molecular shuttle and formation of inclusion complex with the hydrophobic substrate and transferring it to the aqueous media.[29,31,32]

Taking the previous results into account, a novel catalytic system is designed and prepared based on the incorporation of Hal as a filler in a 3D polymeric network, formed from polymerization of CD and glycidyl methacrylate monomer, followed by Pd nanoparticles immobilization. The performance of the catalyst, Pd@Hal-P-CD, was studied for the hydrogenation reaction of nitroarenes. Moreover, comparing the catalytic activity of the catalyst with that of some control catalysts, the roles of Hal, CD and the polymeric network in the catalysis as well as the effect of Hal:CD ratio were investigated. In the following, Pd@Hal-P-CD was carbonized and the catalytic activity of the resulting composite, Pd@Hal-C, was compared with that of Pd@Hal-P-CD. Furthermore, the effect of carbonization temperature on the catalytic activity of the catalyst was studied. In the final section of this research, the recyclability of Pd@Hal-C that exhibited the highest catalytic activity as well as its Pd leaching were examined.

2 | EXPERIMENTAL

2.1 | Materials

The materials applied for the preparation of the catalyst included Hal, β-CD, 3- (trimethoxysilyl) propyl methacrylate (M), potassium peroxide sulphate (KPS), Pd $(OAc)_2$, sodium hydroxide, $NaBH_4$, toluene, distilled water, chloroform and MeOH, all was provided from Sigma-Aldrich and used as received without further purification. The chemicals used for performing the catalytic experiments, i.e. nitroarenes, were purchased from Sigma- Aldrich.

2.2 | Instruments

To characterize the prepared catalyst as well as the control catalysts, the following instruments were applied: XRD, ICP-AES, TGA, BET, TEM, FTIR, Zeta potential and Raman spectroscopy. To record FTIR spectra, PERKIN-ELMER-Spectrum 65 instrument was employed. ICP analyses were performed by using ICP analyzer Varian, Vista-pro. To verify the structure of the catalyst and the control samples, their XRD patterns were recorded using a Siemens, D5000. Cu Kα radiation from a sealed tube. METTLER TOLEDO thermogravimetric analysis apparatus (scanning rate of 10 °C.min^{-1} under N_2 atmosphere) was applied for studying thermal stability of the catalyst. The Raman spectrometer was TEKSAN-N1−541 Spectrum at k = 532 nm instrument. The textural property of the catalyst was investigated by performing BET analysis using a Belsorp Mini II instrument. To prepare the sample for this analysis, the degassing was carried out at 100 °C for 2 hr. Transmission Electron Microscopy (TEM) was accomplished on a Tecnai Microscope (200 kV) to record the morphology of the catalyst and control samples. In detail, the samples were deposited onto a carbon coated copper grid. Pd nanoparticle size distributions have been calculated from the measurement of ~ 200 nanoparticles found in arbitrarily selected area of the images using the program ImageJ. Zeta potential measurements were carried out in water suspension using a Malvern Zetasizer Nano ZS. The calculations are based on a Laser Doppler electrophoretic mobility of metallic nanoparticles via the Helmholtz-Smoluchowski equation, $\xi = (\eta/\epsilon)\mu_e$, where η is the viscosity of the suspending liquid, μ_e is the ratio between the velocity of the nanoparticles and the magnitude under the employed electric field, and ϵ the dielectric conductivity of H_2O. For each test, 5 mg of the composite was dispersed in 5 mL of deionized H_2O and maintained under ultrasonic irradiation for half an hour prior to ZP analysis.

2.3 | Synthesis of the catalyst

2.3.1 | Hal functionalization with 3- (tri-methoxysilyl) propyl methacrylate: Synthesis of Hal-S

To decorate Hal with 3- (tri-methoxysilyl) propyl methacrylate, Hal (1.5 g) was dispersed in dry toluene (40 ml) under ultrasonic irradiation (power of 120 W) for half an hour. Subsequently, 3-(tri-methoxysilyl) propyl methacrylate (1.5 g) was slowly added to the homogenized suspension of Hal in toluene. The resulting mixture was then heated and refluxed under inert atmosphere for 1 day. Upon completion of the reaction, the solid was filtered off, washed with toluene several times and dried in oven at 80 °C for 1 day.

2.3.2 | Polymerization of CD and glycidyl methacrylate in the presence of Hal-S: Synthesis of Hal-P-CD

Hal-S (1.5 g) was first dispersed in the mixture of distilled water and toluene with the aid of ultrasonic irradiation. Then, a solution of CD (5 g in 10 mL distilled water) and KPS (0.1 g) were added to the Hal-S suspension. The obtained mixture was stirred under inert atmosphere for 15 min. Subsequently, M monomer (4 g) was injected to the mixture. Then, the polymerization reaction was carried out at 70 °C for 1 day. At the end of the reaction, the precipitate was collected and washed with distilled water repeatedly. To further purify the product and remove unreacted monomers, the solid was subjected to Soxhlet extraction with chloroform for 72 hr. Finally, the product, Hal-P-CD, was obtained after drying in oven at 80 °C for 12 hr.

2.3.3 | Immobilization of Pd nanoparticles on Hal-P-CD

To immobilize Pd nanoparticles on Hal-P-CD support, Hal-P-CD (7 g) was homogeneously dispersed in dry toluene (30 mL) by using ultrasonic irradiation of power 100 W. Subsequently, a solution of Pd $(OAc)_2$ (0.75 g in 20 ml toluene) as Pd precursor was added to the aforementioned suspension in a dropwise manner. The resulting mixture was then stirred for 1 day. Upon completion of the reaction, a solution of $NaBH_4$ (0.65 g in 30 ml EtOH) was introduced to the mixture in a dropwise manner. After stirring for 1 hr, the precipitate was filtered off, washed and dried at 70 °C in oven for 12 hr.

2.3.4 | Carbonization of Pd@Hal-P-CD: Synthesis of Pd@Hal-C

In the final stage of the synthesis of the catalyst, Pd@Hal-C, the as prepared Pd@Hal-P-CD was carbonized in furnace under inert atmosphere for 4.5 hr (the first 4 hr at 450 °C and the last 2 hr at 750 °C). The schematic representation of the procedure used for the synthesis of the catalyst, Pd@Hal-C, is depicted in Figure 1. Using ICP analysis, the content of Pd in Pd@Hal-C was calculated to be 0.19 $mmol.g^{-1}$.

It is worth noting that for the synthesis of the control catalysts, Pd@Hal, Pd@P, Pd@P-CD, Pd@Hal-CD, Pd@Hal-P, the same procedure was used, except Hal, P and P-CD were applied as catalyst support, respectively. Moreover, to elucidate the role of the ratio of the monomers in the catalysis, Pd@Hal-P-CD catalyst with CD:M ratio of 6:3 was also prepared. To study the effect of carbonization temperature, apart from the main catalyst that was carbonized at 450−750 °C (Pd@Hal-C750), another catalyst (Pd@Hal-C600) was prepared, in which carbonization was performed at 450−600 °C.

2.4 | Hydrogenation reaction

The hydrogenation of nitro compounds and formation of the corresponding anilines was carried out as follow: the catalyst (3 wt. %) was introduced to the mixture of nitro compound (1 mmol) in deionized water (2 ml) in a glass reactor. Then, the temperature of the mixture was elevated to 60 °C and hydrogen gas was purged into the reaction vessel (H_2 pressure of 1 atm). After that, the mixture was stirred vigorously (700 rpm) and the progress of the reaction was monitored via TLC. At the end of the reaction, the catalyst was separated via simple filtration, washed with H_2O for several times and dried at 95 °C overnight for reusing in the consecutive reaction runs. To obtain the anilines, the solvent was evaporated. To identify the organic products, their melting/boiling point and FTIR spectra were compared with those of the authentic samples.

3 | RESULTS AND DISCUSSION

3.1 | Catalyst characterization

To verify the formation of the Pd@Hal-P-CD as well as Pd@Hal-C, their FTIR spectra were recorded (Figure 2). As depicted, the FTIR spectrum of Pd@Hal-P-CD exhibited the characteristic bands at 1729 cm^{-1} that can be assigned to the −C=O functionality in the backbone of the P, 3440 cm^{-1} that can be due to the −OH functionality

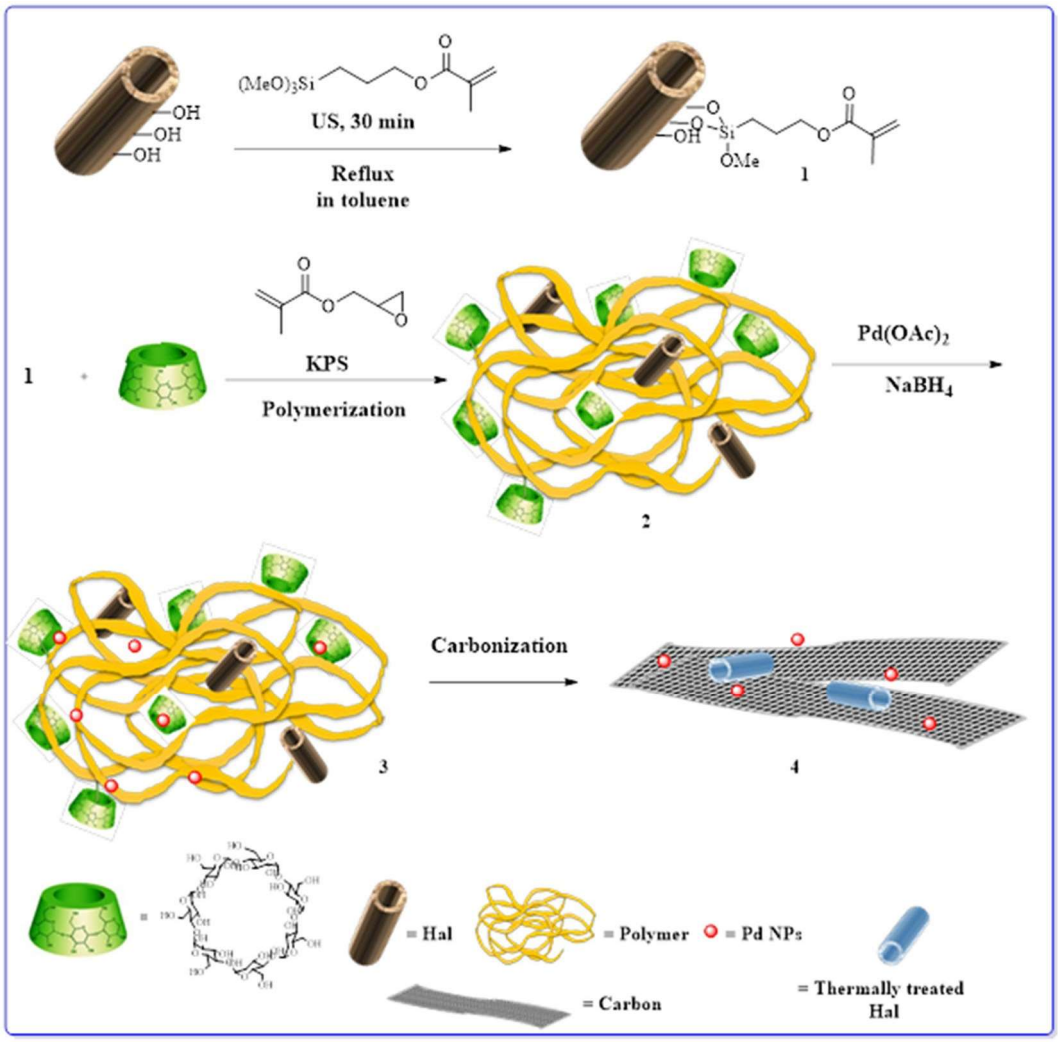

FIGURE 1 The schematic representation of the procedure used for the synthesis of the catalyst

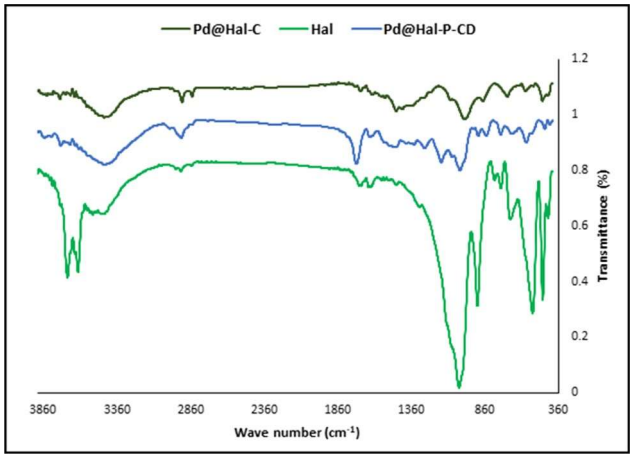

FIGURE 2 FTIR spectra of Hal, Pd@Hal-P-CD and Pd@Hal-C

of CD as well as the hydroxyl groups of the opened epoxy rings and 2925 cm^{-1} (-CH_2 stretching). Noteworthy, the short characteristic bands at 1027 cm^{-1} and 580 cm^{-1} can also be observed that can be attributed to the Si−O stretching and Al-O-Si vibration of the incorporated Hal respectively (Figure 2). Moreover, the two small bands at 3737 and 3675 cm^{-1} can be assigned to the internal hydroxyl groups of Hal. Other characteristic bands of Hal overlapped with that of P-CD.[33] The formation of Pd@Hal-C can be confirmed by comparing the FTIR spectrum of the catalyst with that of Pd@Hal-P-CD. More precisely, the disappearance of the characteristic band of P (the band at 1729 cm^{-1}) can indicate the successful carbonization. The bands at 2925 cm^{-1} and 3440 cm^{-1} in the FTIR spectrum of Pd@Hal-C can be attributed to the −CH_2 and −OH functionalities in C. Noteworthy, the Hal characteristic band at 1027 cm^{-1} is shifted to 1091 cm^{-1}, indicating the coverage of Al in Hal structure with carbon.[34] Moreover, the band at 910 cm^{-1} that is indicative of Al-OH bending vibration disappeared in the FTIR spectrum of Pd@Hal-C. This can be attributed to the thermal treatment of Hal-P-CD.[34]

To further characterize the catalyst, the TGA thermogram of Pd@Hal-C was recorded and compared with that

of pristine Hal and Pd@Hal-P-CD (Figure 3). The weight losses in the thermogram of pristine Hal included the loss at ~140 °C that is due to the loss of water in Hal structure and the loss related to the Hal dehydroxylation (~540 °C).[35,36] As illustrated, Hal-P-CD exhibited lower thermal stability compared to Hal. In more detail, besides loss of water (at ~ 100 °C), two more losses were observed at 290 (19.5 wt.%) and 380 °C (37.9 wt.%). These weight losses can be assigned to the degradation of P-CD. As shown in (Figure 3), upon carbonization and formation of Pd@Hal-C, the thermal stability significantly increased. This observation can further confirm the successful carbonization of P-CD.

To shed more light to the structure of the catalyst, the XRD patterns of pristine Hal, Pd@Hal-P-CD and Pd@Hal-C were recorded and compared (Figure 4). As illustrated in Figure 4, in the XRD pattern of Pd@Hal-C, the characteristic bands of Hal (2θ = 11.5°, 20.2°, 26.7°, 35.4°, 55.6° and 62.1°, JCPDS No. 29−1487 (labelled as H)) can be observed.[37,38] However, the intensities of these peaks are dramatically decreased and small shift can also be seen. According to the literature, the decrease in the intensity of Hal characteristic bands can be assigned to the thermal treatment.[34,39] On the other hand, the slight shift of the Hal characteristic bands can be attributed to the intercalation of P chain between the silicate layers of Hal.[40] Moreover, the Pd characteristic bands can be observed at 2θ = 41.1 °, 45.5°, 68.7°, 79.6°, and 87° (labelled as P) that can be assigned to the {111},[41] {200}, {220}, {311} and {222} planes of Pd (JCPDS, No.46−1043).[42] Apart from Hal and Pd characteristic bands, an additional band at 2θ = 24.2° appeared and that can be attributed to the formation of graphite-like carbon structure (crystalline carbon).[43] Regarding Pd@Hal-P-CD, only a broad band at 2θ = 13−20° can be detected in the XRD pattern that can be assigned to the amorphous P-CD. The absence of the characteristic bands of Hal and Pd can be attributed their low content in the composite.[44]

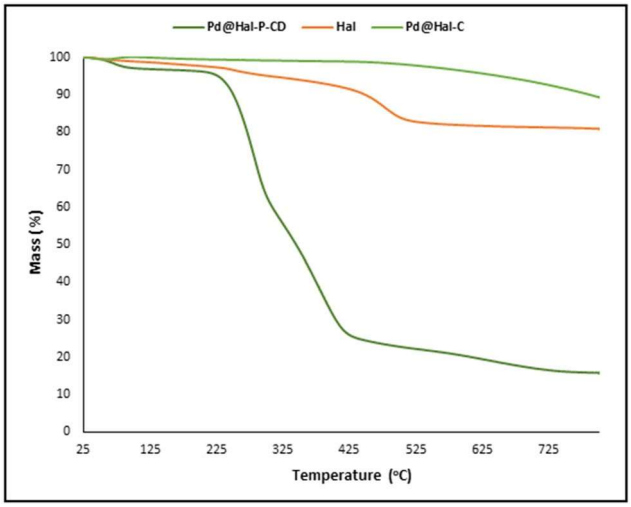

FIGURE 3 TGA thermograms of Hal, Pd@Hal-P-CD andPd@Hal-C

The N_2-adsorption−desorption isotherm of Pd@Hal-C, depicted in Figure S1, exhibited type IV isotherm, indicating the porous nature of Pd@Hal-C. The BET analysis showed that the specific surface area of the catalyst was 193 m^2 g^{-1}.

In order to have a better idea of the dispersion and the size of Pd nanoparticles dispersed onto the support, TEM characterization of the different synthesized samples has been done. First, the TEM images of Pd@Hal clearly show that the structure of the Hal nanotubes is preserved after the deposition of the metal nanoparticles (The Pd nanoparticles are deposited on the Hal tubes, Figure S2). Nevertheless, the dispersion of the Pd nanoparticles onto the support is not so good even if no aggregation is observed. If Pd nanoparticles were supported on the

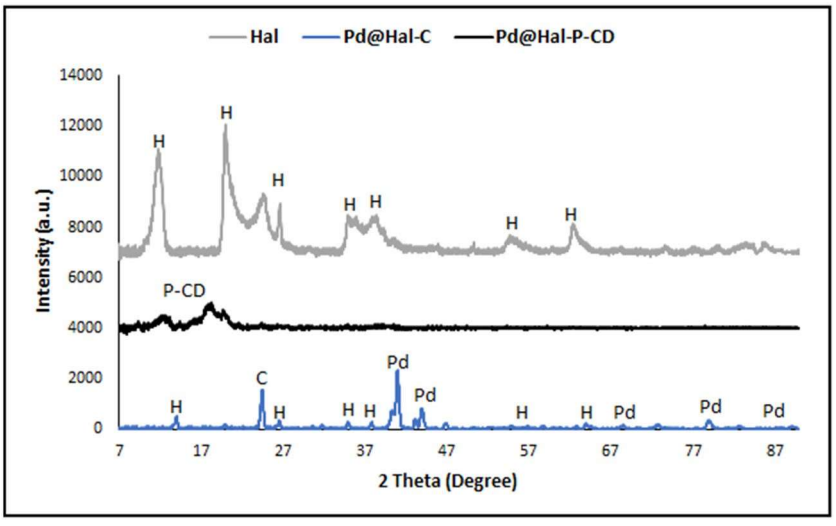

FIGURE 4 XRD patterns of Hal,Pd@Hal-P-CD and Pd@Hal-C

Hal-P-CD polymer, considering a CD:M molar ratio of 5:4, a good dispersion of Pd nanoparticles is observed with a mean diameter of 6.6 ± 3.2 nm (Figure 5 and Figure S3). As shown in Figure 5, the Pd nanoparticles (black spots) can be observed on the polymeric sheet. This better dispersion of Pd nanoparticles could be explained by the strongest interaction between the Pd metallic salt and the Hal-P-CD polymer in the organic phase. It should be noticed that it is not possible to see the structure of Hal nanotube in this sample coming from the fact that the Hal is well embedded in P-CD polymer. If the CD:M molar ratio is increased from 5:4 to 6:3, the dispersion of Pd nanoparticles is greatly altered (Figure S4). Indeed, large aggregates are observed and consequently, a poor dispersion of Pd nanoparticles is obtained. Pd@Hal-C was furnished from the carbonization at 750 °C of Pd@Hal-P-CD and the TEM characterization clearly showed that the carbonization resulted in the increase of the size of the Pd nanoparticles. In the TEM images of this catalysts, the large Pd nanoparticles on the carbon sheet are observable. Indeed, the mean diameter of the Pd nanoparticles increased from 6.6 ± 3.2 nm to 26.0 ± 12.6 nm (Figure S5) keeping the good dispersion of Pd nanoparticles onto the support. It was found that in the sample with higher amount of CD in P-CD, the increase of the size of Pd nanoparticles after the carbonization step was less pronounced (with final mean diameter of 20.9 ± 15.2 nm, Figure S6) with a good dispersion of Pd nanoparticles onto the support.

The increase of the hydrophobicity of the material after the carbonization step has also been confirmed by zeta potential measurement (Figure S7). Indeed, the zeta potential value of Pd@Hal dispersion is about −45.8 mV. This value is classical for a Hal support dispersed into water because of the negative charge on the outer surface of this material. This value for Pd@Hal-P-CD was about −47.5 mV, very similar to that of Pd@Hal. Nevertheless, after the carbonization step, this zeta potential is decreasing from −47.5 to −38.6 mV. This decrease could be explained by the increase of the hydrophobicity of the surface of the catalyst coming from the formation of a carbon layer onto the Hal surface.

3.2 | Catalyst activity

Encouraged by the results of our previous report,[30] in which Hal-P showed high performance as catalyst support, a novel catalytic system was designed. On the contrary of the previous report that polymer covered Hal tubes, in this study a polymeric network was targeted, in which Hal tubes were dispersed through covalent bonding. Another novelty of the presented catalyst was

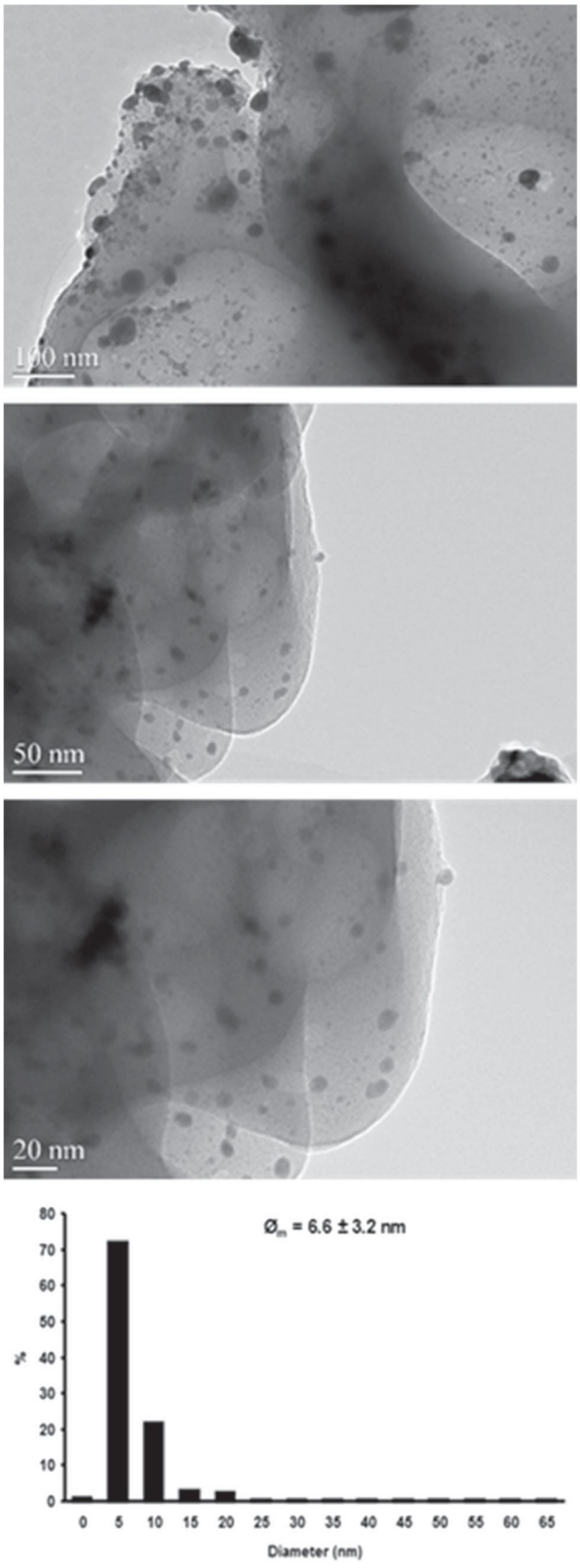

FIGURE 5 TEM images at different magnifications and size distribution of Pd@Hal-P-CD catalyst

incorporation of CD as co-monomer and formation of a co-polymer of P-CD. The aim of this design was benefiting from the capability of CD for the encapsulation of the hydrophobic substrate and serving as phase transfer agent to make the reaction possible in aqueous media.

To investigate the catalytic activity of the catalyst, the hydrogenation of nitrobenzene was targeted as a model catalytic reaction. Initially, the reaction variables were optimized by studying their effects on the reaction yield (Table S1). The optimization tests showed that performing hydrogenation in the presence of catalytic amount of Pd@Hal-P-CD (3 wt.%) in water as solvent at 60 °C and hydrogen gas as reducing agent resulted in a conversion of 80% and a selectivity of 100% towards aniline after 75 min.

Armed with the optimum reaction condition and with the aim of studying the contribution of P, CD and Hal, several control catalysts including, Pd@P, Pd@Hal, Pd@Hal-P, Pd@P-CD and Pd@Hal-CD were synthesized and their catalytic activities for promoting hydrogenation of nitrobenzene were compared with that of Pd@Hal-P-CD (Table 1).

As shown in Table 1, the catalytic activity of Pd@Hal was insignificant (Entry 8, Table 1). This observation was quite expectable as bare Hal cannot effectively immobilize Pd nanoparticles.[5] The catalytic activity of Pd@P (Entry 9, Table 1) was also very low, but higher than that of Pd@Hal. The higher activity of Pd@P could be attributed to the presence of several functionalities in the backbone of polymer network that could act as anchors for Pd nanoparticles. The catalytic activity of Pd@Hal-P (Entry 5, Table 1) was superior compared to Pd@Hal and Pd@P, confirming the positive effect of composite formation of Hal and P on the catalytic activity of the resulting catalyst. According to the literature, this could stem from the synergism between two components of the composite.[27] Interestingly, Pd@Hal-P-CD (Entry 3, Table 1) exhibited high catalytic activity that was remarkably superior compared to that of three above-mentioned catalysts. According to the literature, this observation can be assigned to the role of CD as a phase transfer agent and its capability to form inclusion complex with the hydrophobic substrate and transfer it to the aqueous media.[15–17] Moreover, CD can induce its effect through acting as capping agent for Pd nanoparticles and preventing them from aggregation. This can be confirmed from TEM results that showed Pd nanoparticle with mean diameter of 6.6 ± 3.2 nm and good dispersion.

TABLE 1 The comparison of the catalytic activity of the catalyst for hydrogenation of nitrobenzene with that of control samples[a]

Entry	Catalyst	Yield. [%][b]
1	Pd@Hal-C750	100
2	Pd@Hal-C[c]	60
3	Pd@Hal-P-CD	80
4	Pd@Hal-P-CD[d]	50
5	Pd@Hal-P	35
6	Pd@Hal-CD	35
7	Pd@P-CD	22
8	Pd@Hal	10
9	Pd@P	20
10	Pd@Hal-C600[e]	92

[a]Reaction conditions: Substrate (1 mmol), catalyst (3 wt%), H_2O (2 ml), agitation (700 rpm) at 60 °C.

[b]Isolated yields.

[c]The catalyst prepared by carbonization of Pd@Hal-P-CD synthesized by using CD:M ratio of 6:3.

[d]Pd@Hal-P-CD prepared by using CD:M ratio of 6:3.

[e]The catalyst prepared via carbonization at lower temperature (450−600 °C).

To further investigate the contribution of CD to the catalysis, Pd@Hal-CD (Entry 6, Table 1) and Pd@P-CD (Entry 7, Table 1) were also prepared and their catalytic activities were compared with that of the CD-free counterparts. As tabulated, the catalytic activity of Pd@Hal-CD was superior to that of Pd@Hal catalyst, emphasizing the role of CD in the catalysis. Notably, this effect was not pronounced in the case of Pd@P-CD.

Confirming the contribution of CD to the catalysis, the effect of the content of CD on the catalyst backbone was studied by changing the ratio of CD: M monomer in the course of formation of Pd@Hal-P-CD. In this line, two catalysts with the ratios of 5:4 and 6:3 of CD:M were prepared (Entries 3 and 4, Table 1) and their catalytic activities were examined. The results showed that the optimum ratio of CD:M was 5:4 and increase of this ratio to 6:3 decreased the catalytic activity. This issue can be justified by the TEM results. As discussed above, increase of CD:M from 5:4 to 6:3 resulted in large aggregates and consequently, a poor dispersion of Pd nanoparticles. This can lead to the inferior catalytic activity. This observation can show that there is an optimum amount for the content of CD and further increase of this value can have a converse effect on the observed catalytic activity.

Motivated by the previous results on the high catalytic activity of Hal-carbon composites,[28,32] in the second part of this study, it was elucidated whether carbonization of Pd@Hal-P-CD has a positive effect on the catalytic activity of the catalyst. In this line, Pd@Hal-P-CD was carbonized, characterized and the catalytic activity of the resulting catalyst, Pd@Hal-C, for promoting the hydrogenation of the model reaction under similar reaction condition was measured (Entry 1, Table 1) and compared with that of Pd@Hal-P-CD. Notably, the characterization of Pd@Hal-C showed that carbonization resulted in significant

change in the structure of the catalyst. More precisely, upon carbonization, the Hal structure was affected and partially destructed (as shown in the XRD pattern). On the other hand, due to the low yield of carbonization (about 20%), the content of Pd in the Pd@Hal-C increased significantly compared to that of Pd@Hal-P-CD (almost four fold). Consequently, for the same catalyst weight, the amount of Pd is higher with Pd@Hal-C than with Pd@Hal-P-CD. However, carbonization resulted in the aggregation of Pd nanoparticles to some extent and increase of the Pd nanoparticles mean size (Figure S5). Moreover, the thermal stability of the catalyst as well as its hydrophobicity increased (Figure S7). All of these changes can affect the catalytic activity and their combinational effects led to the increase of the catalytic activity of Pd@Hal-C compared to its non-carbonized counterpart.

Considering these results and in attempt to clarify whether incorporation of Hal in the structure of Pd@Hal-C has any contribution to the catalysis, carbonization of Hal free sample, i.e. Pd@P-CD, was performed to see whether Hal-free catalyst could lead to a catalyst with similar catalytic activity. To this purpose, CD and M monomer were polymerized in the absence of Hal and then carbonized and used as a catalyst for promoting the model reaction. It was found that the presence of Hal could both improve the yield of polymerization and the catalytic activity of the resulting catalyst. According to the literature, this observation can be attributed to the effect of Hal on the resulting polymer.[45,46] Hence, although Hal is partially destroyed in the course of carbonization, its incorporation was beneficial for achieving the best catalytic activity.

Notably, the carbonization of Pd@Hal-P-CD with higher content of CD (Entry 2, Table 1) led to a catalyst with moderate catalytic activity. This result further confirmed the importance of ratio of CD:M on the catalytic activity. Moreover, according to the literature, this observation can be assigned to the effect of CD as precursor on the nature of the final carbon.[20]

Finally, the effect of carbonization condition on the catalytic activity of the resulting catalyst was studied by comparing the catalytic activity of Pd@Hal-C600 and Pd@Hal-C750 (Table 1, entries 10 and 1). As tabulated, the carbonization temperature can affect the catalytic activity and Pd@Hal-C750 exhibited higher catalytic activity.

To further investigate the effect of carbonization temperature, the TGA thermogram of Pd@Hal-C600 and Pd@Hal-C750 were compared (Figure 6). As shown, the thermal stability of Pd@Hal-C750 was higher than that of Pd@Hal-C600. In the TGA thermogram of Pd@Hal-C600, an additional loss stage can be detected at 310 °C, indicating that carbonization of P-CD cannot be completed by treatment at 600 °C and the degradation of the remaining P-CD resulted in the observed loss stage.

It was assumed that carbonization can influence the nature of the resultant carbon. To verify this postulate, the Raman spectra of both samples were recorded and compared (Figure 7). As depicted, in the Raman spectra of two samples two bands, a D-band at 1327 cm^{-1} and a G-band at 1615 cm^{-1}, can be observed. According to the literature, the D band can be indicative of the sp^3 configuration that can be attributed to presence of intrinsic defects and the G-band is due to the graphitic carbon.[47–49] The comparison of two Raman spectra showed that the I_D/I_G value for Pd@Hal-C600 and Pd@Hal-C750 were 0.92 and 0.84 respectively. This result can indicate that the C obtained at elevated temperature has more graphitic nature.

Noteworthy, the XRD pattern of Pd@Hal-C600 is distinguishable from Pd@Hal-C750 (Figure 8). More precisely, in the XRD pattern of Pd@Hal-C600, a band at 2θ = 20–22.8° can be observed. According to the previous reports, the observed broad band can be assigned to the (002) reflection of C, implying that the catalyst can also contain a number of amorphous compounds.[50] Comparing the C characteristic bands in two XRD patterns of Pd@Hal-C600 (the broad band at 2θ = 20–22.8° and a small band at 2θ = 25°) and Pd@Hal-C750 (a sharp band at 2θ = 25°), it can be concluded that the natures of C in these samples are different. This issue was further confirmed via Raman spectroscopy.

On the other hand, in the XRD pattern of Pd@Hal-C600, the Hal characteristic bands are more pronounced compared to Pd@Hal-C750. This observation is in good agreement with the literature,[34,39] in which it was confirmed that the disappearance of Hal characteristic bands is pronounced upon thermal treatment at elevated temperatures.

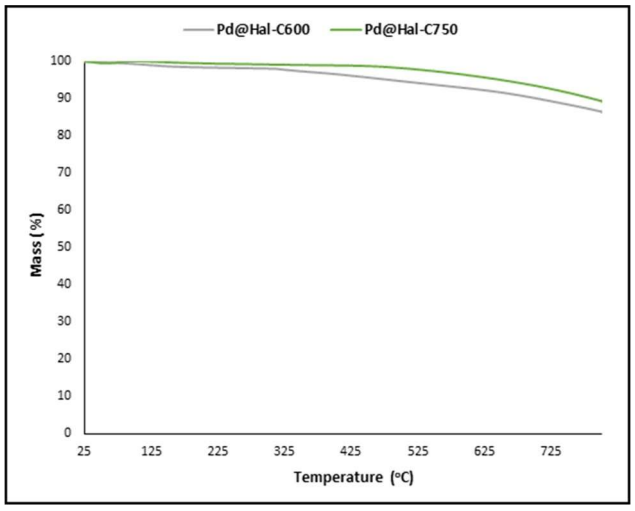

FIGURE 6 TGA thermograms of Pd@Hal-C600 and Pd@Hal-C750

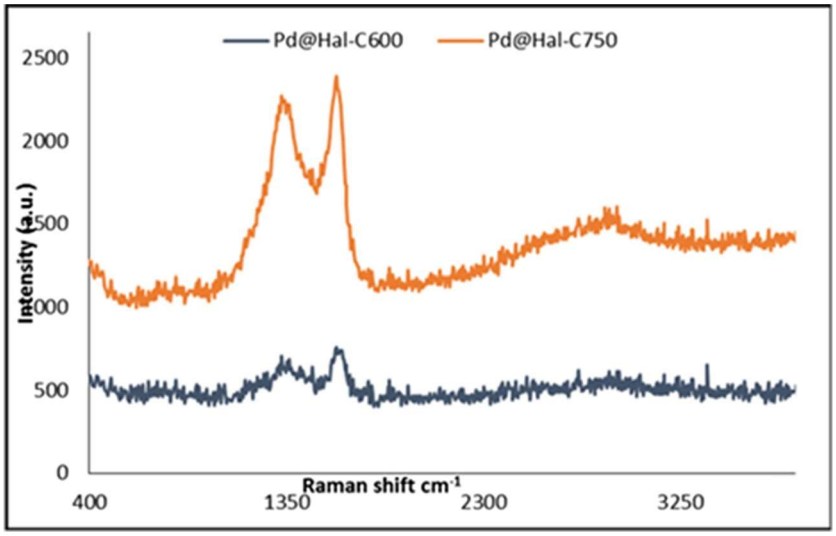

FIGURE 7 The Raman spectra Pd@Hal-C600 and Pd@Hal-C750

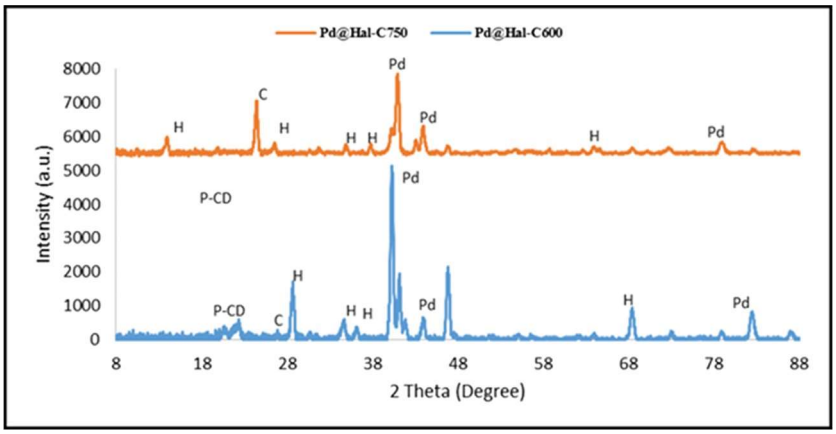

FIGURE 8 XRD patterns of Pd@Hal-C600 and Pd@Hal-C750

Measurement of the zeta potential value of Pd@Hal-C750 and Pd@Hal-C600 (Figure S7) showed that this value for Pd@Hal-C600 was slightly higher (−33.4 mV) than that of Pd@Hal-C750.

Finding Pd@Hal-C as the best catalyst, the selectivity of the catalyst towards nitro reduction was studied. To this purpose, 4-nitroacetophenone was hydrogenated as a substrate with two functional groups. Gratifyingly, the result showed that 4-nitroacetophenone underwent the hydrogenation reaction to afford 4-aminoacetophenone as a sole product. Although the yield of this reaction was lower (80%) than that of the model one, observation of no by-product can confirm high selectivity of the catalyst towards nitro group.

In the next step, the catalytic activity of Pd@Hal-C was compared with some of previously reported catalysts reported for the hydrogenation of nitrobenzene (the model substrate), Table 2. As tabulated, this reaction has been subjected to numerous studies and various catalysts have been applied for promoting this hydrogenation reaction using different reducing agents, including hydrogen gas and chemical reducing agents under different reaction conditions. The catalysts tabulated in Table 2 exhibited high catalytic activities for hydrogenation of nitrobenzene. However, some of the reported catalysts are efficient at high H_2 pressure. On the other hand, in some of the listed procedures chemical reducing agents or toxic organic solvents are used. Taking the environmental issues into account, use of low pressure of hydrogen gas as hydrogen source is more appealing. Furthermore, use of water as environmentally benign solvent renders the reaction more promising. Considering these points as well as high catalytic activity and recyclability of Pd@Hal-C, it can be concluded that this catalyst can be classified as one of the efficient catalysts with utility for the hydrogenation of nitroarenes.

3.3 | Catalyst recyclability

Confirming high catalytic activity of the catalyst, it was studied whether Pd@Hal-C was a recyclable catalyst. In

TABLE 2 The comparison of the catalytic activities of Pd@Hal-C with some of previously reported catalysts for the hydrogenation of nitrobenzene

Entry	Catalyst	Temperature (°C)	Solvent	Time (h:min)	Reducing agent	Yield (%)	Ref
1	Pd@Hal-C750 (3 wt%)	60	H_2O	1:15	H_2/1 atm	100	This work
2	Pd@Hal/di-urea[a] (1.5 wt%)	50	H_2O	1:00	H_2/1 bar	100	[52]
3	Pd/PPh_3@FDU-12[b] (8.33×10^{-4} mmol Pd)	40	EtOH	1:00	H_2/10 bar	99	[53]
4	PdNP(0.5%)/Al_2O_3 (0.3 g)	r.t.	THF	3:00	H_2/1 atm	100	[54]
5	APSNP[c] (1 mol%)	r.t.	EtOH	2:00	H_2/40 atm	100	[55]
6	Pd-$(CH_3)_2NHBH_3$ (6 mol%)	r.t.	H_2O/MeOH	0:10	$(CH_3)_2NHBH_3$	99	[56]
7	Pd/graphene	50	H_2O/EtOH	1:30	$NaBH_4$	91	[57]
8	Pd0-AmP-MCF[d] (0.5 mol%)	r.t	EtOAc	1.15	H_2/1 bar	90	[58]
9	Pd NPs/RGO (6 mg)	50	H_2O/EtOH	1:30	$NaBH_4$	98	[59]
10	PdNP@PPh_2-PEGPIILP[e] (0.05 mol%	r.t.	H_2O	2:00	$NaBH_4$	99	[60]
11	PdCu/graphene (2 mol% Pd)	50	H_2O/EtOH	1:30	$NaBH_4$	98	[57]
12	PdCu/C (2 mol% Pd)	50	H_2O/EtOH	1:30	$NaBH_4$	85	[57]

[a]Pd immobilized on functionalized Hal

[b]Pd NPs (1.1 nm) with triphenylphosphine (PPh3) cross-linked in the nanopore of FDU-12

[c]activated palladium sucrose nanoparticles

[d]Pd nanoparticles supported on aminopropyl-functionalized siliceous mesocellular foam

[e]Palladium nanoparticles stabilized by lightly cross-linked phosphine-decorated polymer immobilized ionic liquids (PIIL) and their PEGylated counterparts (PEGPIIL)

this line, at the end of the hydrogenation reaction of nitrobenzene in the presence of fresh Pd@Hal-C, the catalyst was simply separated from the reaction mixture and washed. After drying in oven at 90 °C, the recovered catalyst was subjected to the next run of hydrogenation reaction under similar reaction conditions. The recovery-reusing cycle was repeated for 6 reaction runs and the yield of aniline after each recycling was calculated and compared with that of the fresh Pd@Hal-C. The results (Figure 9) exhibited that Pd@Hal-C could be successfully recycled for five reaction runs with slight loss of activity. However, further recycling up to sixth reaction run led to the significant loss of the catalytic activity.

To further investigate the effect of recycling on Pd@Hal-C, the recycled Pd@Hal-C after 6 reaction runs was characterized with TEM, ICP and FTIR spectroscopy. The ICP analysis showed that recycling of the catalyst for 5 times led to the low Pd leaching. However, this value reached to its maximum point (7 wt% initial Pd loading) upon sixth recycling. The FTIR spectrum

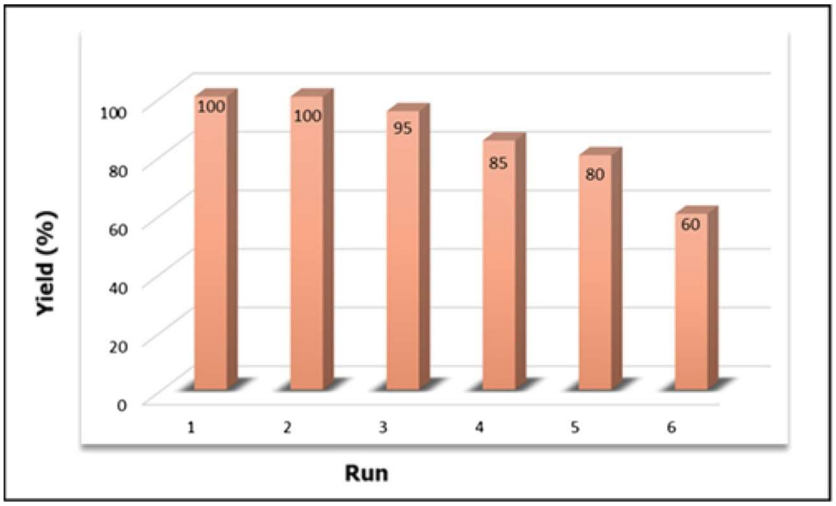

FIGURE 9 The recycling result ofPd@Hal-C750 catalyst

of the recycled Pd@Hal-C (Figure 10) confirmed the structural stability of the catalyst in the course of the reaction. More precisely, the FTIR spectrum of the recycled catalyst exhibited the characteristic bands of the fresh catalyst.

It should be noticed that the TEM characterization of the recycled catalyst has been performed (Figure S8). No aggregation of Pd nanoparticles was observed onto the support after several runs and moreover, the size of Pd nanoparticles was not greatly altered after the 6th run with a mean diameter about 27.2 ± 10.7 nm. This analysis is a proof that the Pd nanoparticles are efficiently adsorbed onto the composite.

3.4 | Hot filtration test

The last part of this study was dedicated to the investigation of the nature of the catalyst species. To this purpose, conventional hot filtration test was performed.[51] Briefly, the catalyst was removed from the reaction mixture after a short reaction time and the progress of the hydrogenation reaction was monitored in the filtrate. As the reaction did not proceed in the absence of the catalyst, it can be concluded that the true catalyst was heterogeneous and did not proceed through Pd leaching and re-deposition.

4 | CONCLUSIONS

With the aim of taking advantage of Hal, P and CD chemistry, a novel composite, Pd@Hal-P-CD, was prepared by polymerization of β-CD and M monomer in the presence of functionalized Hal, followed by Pd immobilization. The resulting nanocomposite showed high catalytic activity for promoting hydrogenation reaction of nitrobenzene in aqueous media, superior compared to that of Pd@Hal-P, Pd@Hal-CD, Pd@P-CD, Pd@Hal and Pd@P. It was postulated that CD could act not only as a phase transfer agent, but also as a capping agent for the Pd nanoparticles. Moreover, the synergism between the components could improve the catalytic activity of the nanocomposite compared to the individual components. It was also confirmed that the ratio of the monomers played an important role in the Pd particle size and the catalytic activity of the final catalyst. The carbonization of Pd@Hal-P-CD was also carried out to afford a new composite, Pd@Hal-C that exhibited superior catalytic activity compared to Pd@Hal-P-CD. Characterization of Pd@Hal-C confirmed significant structural change such as growth of Pd nanoparticles, increase of Pd content and partial destruction of Hal upon carbonization. The study on the carbonization temperature indicated that carbonization at elevated temperature could lead to the formation of a catalyst with higher catalytic activity. It was also found out that although Hal was partially destroyed in Pd@Hal-C, its presence in the backbone of the catalyst could improve the catalytic activity.

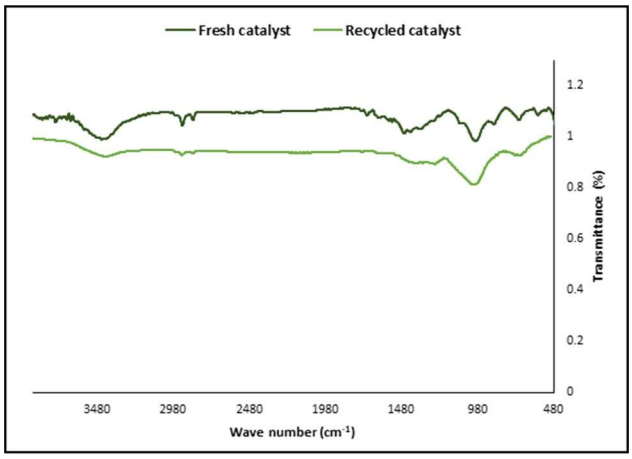

FIGURE 10 FTIR spectra of fresh and recycled catalyst

ACKNOWLEDGMENTS

The TEM in Lille (France) are supported by the Conseil Régional du Nord-Pas de Calais and the European Regional Development Fund (ERDF). This work has been supported by the Center for International Scientific Studies & Collaborations (CISSC) and French Embassy in Iran and Hubert Curien French-Iranian partnership "PHC GUNDISHAPUR 2018" n° 40870ZG. S. Sadjadi appreciate Iran National Science Foundation for the Individual given grant, No. 97009384.

CONFLICT OF INTEREST

There are no conflicts to declare. The Iranian authors declare that none of them are employed by a government agency that has a primary function other than research and/or education. Moreover, none of them are official representative or on behalf of the government.

ORCID

Samahe Sadjadi https://orcid.org/0000-0002-6884-4328
Bastien Léger https://orcid.org/0000-0003-2411-1162
Eric Monflier https://orcid.org/0000-0001-5865-0979

REFERENCES

[1] Y. Lvov, A. Panchal, Y. Fu, R. Fakhrullin, M. Kryuchkova, S. Batasheva, A. Stavitskaya, A. Glotov, V. Vinokurov, *Langmuir* **2019**, *35*, 8646.

[2] Y. Lvov, W. Wang, L. Zhang, R. Fakhrullin, *Adv. Mater.* **2016**, *28*, 1227.

[3] Y. Zhao, W. Kong, Z. Jin, Y. Fu, W. Wang, Y. Zhang, J. Liu, B. Zhang, *Appl. Energy* **2018**, *222*, 180.

[4] M. Massaro, C. G. Colletti, G. Buscemi, S. Cataldo, S. Guernelli, G. Lazzara, L. F. Liotta, F. Parisi, A. Pettignano, S. Riela, *New J. Chem.* **2018**, *42*, 13938.

[5] M. Massaro, C. G. Colletti, G. Lazzara, S. Milioto, R. Noto, S. Riela, *J. Mater. Chem. A* **2017**, *5*, 13276.

[6] Y. Liu, J. Zhang, H. Guan, Y. Zhao, J.-H. Yang, B. Zhang, *Appl. Surf. Sci.* **2018**, *427*, 106.

[7] S. Li, F. Tang, H. Wang, J. Feng, Z. Jin, *RSC Adv.* **2018**, *8*, 10237.

[8] M. Mahdavi, H. Lijan, S. Bahadorikhalili, L. Ma'mani, P. Rashidi Ranjbar, A. Shafiee, *RSC Adv.* **2016**, *6*, 28838.

[9] W.-N. Xing, L. Ni, X.-S. Yan, X.-L. Liu, Y.-Y. Luo, Z.-Y. Lu, Y.-S. Yan, P.-W. Huo, *Acta Phys.-Chim. Sin.* **2014**, *30*, 141.

[10] L. Jiang, Y. Huang, T. Liu, *J. Colloid Interface Sci.* **2015**, *439*, 62.

[11] W. Ma, H. Wu, Y. Higaki, A. Takahara, *Chem. Rec.* **2018**, *18*, 1.

[12] V. Vinokurov, A. Glotov, Y. Chudakov, A. Stavitskaya, E. Ivanov, P. Gushchin, A. Zolotukhina, A. Maximov, E. Karakhanov, Y. Lvov, *Ind. Eng. Chem. Res.* **2017**, *56*, 14043.

[13] N. Bahri-Laleh, S. Sadjadi, A. Poater, *J. Colloid Interface Sci.* **2018**, *531*, 421.

[14] M. Massaro, V. Schembri, V. Campisciano, G. Cavallaro, G. Lazzara, S. Milioto, R. Noto, F. Parisi, S. Riela, *RSC Adv.* **2016**, *6*, 55312.

[15] F. Hapiot, H. Bricout, S. Menuel, S. Tilloy, E. Monflier, *Cat. Sci. Technol.* **2014**, *4*, 1899.

[16] F. Hapiot, E. Monflier, *Catalysts* **2017**, *7*, 173.

[17] D. Prochowicz, A. Kornowicz, J. Lewiński, *Chem. Rev.* **2017**, *117*, 13461.

[18] Y.-Y. Chu, Z.-B. Wang, Z.-Z. Jiang, D.-M. Gu, G.-P. Yin, *Adv. Mater.* **2011**, *23*, 3100.

[19] W. Zhu, T. Liu, W. Chen, X. Liu, *Mater. Lett.* **2015**, *139*, 122.

[20] E. S. Da Silva, N. M. M. Moura, A. Coutinho, G. Drazic, B. M. S. Teixeira, N. A. Sobolev, C. G. Silva, M. G. Neves, M. Prieto, J. L. Faria, *ChemSusChem* **2018**, *11*, 2681.

[21] E. A. Gelder, S. D. Jackson, C. M. Lok, *Chem. Commun.* **2005**, 522.

[22] N. Bouchenafa-Saib, P. Grange, P. Verhasselt, F. Addoun, V. Dubois, *Appl. Catal., A* **2005**, *286*, 167.

[23] X. Yu, M. Wang, H. Li, *Appl. Catal., a* **2000**, *202*, 17.

[24] R. Giordano, P. Serp, P. Kalck, Y. Kihn, J. Schreiber, C. Marhic, J. L. Duvail, *Eur. J. Inorg. Chem.* **2003**, *2003*, 610.

[25] C.-H. Li, Z.-X. Yu, K.-F. Yao, S.-f. Ji, J. Liang, *J. Mol. Catal. A: Chem.* **2005**, *226*, 101.

[26] N. Arora, A. Mehta, A. Mishra, S. Basu, *Appl. Clay Sci.* **2018**, *151*, 1.

[27] S. Sadjadi, M. Atai, *Appl. Clay Sci.* **2018**, *153*, 78.

[28] S. Sadjadi, G. Lazzara, M. Malmir, M. M. Heravi, *J. Catal.* **2018**, *366*, 245.

[29] S. Sadjadi, M. Akbari, E. Monflier, M. M. Heravi, B. Leger, *New J. Chem.* **2018**, *42*, 15733.

[30] S. Sadjadi, F. Koohestani, N. Bahri-Laleh, K. Didehban, *J. Solid State Chem.* **2019**, *271*, 59.

[31] S. Sadjadi, *Appl. Organomet. Chem.* **2018**, *32*, 4211.

[32] S. Sadjadi, M. M. Heravi, M. Malmir, *Carbohydr. Polym.* **2018**, *186*, 25.

[33] S. Sadjadi, M. M. Heravi, M. Malmir, *Res. Chem. Intermed.* **2017**, *43*, 6701.

[34] J. Jin, L. Fu, C. Yang, J. Ouyang, *Sci. Rep.* **2015**, *5*, 1.

[35] S. Bordeepong, D. Bhongsuwan, T. Pungrassami, T. Bhongsuwan, *Songklanakarin J. Sci. Technol.* **2011**, *33*, 599.

[36] L. Zatta, J. E. F. da Costa Gardolinski, F. Wypych, *Appl. Clay Sci.* **2011**, *51*, 165.

[37] H. Zhu, M. L. Du, M. L. Zou, C. S. Xu, Y. Q. Fu, *Dalton Trans.* **2012**, *41*, 10465.

[38] P. Yuan, P. D. Southon, Z. Liu, M. E. R. Green, J. M. Hook, S. J. Antill, C. J. Kepert, *J. Phys. Chem. C* **2008**, *112*, 15742.

[39] J. Zhang, B. Mu, A. Wang, *J. Solid State Electrochem.* **2015**, *19*, 1257.

[40] C. E. Yeniova Erpek, G. Ozkoc, U. Yilmazer, *Polym. Compos.* **2017**, *38*, 2337.

[41] G. Lazzara, G. Cavallaro, A. Panchal, R. Fakhrullin, A. Stavitskaya, V. Vinokurov, Y. Lvov, *Curr. Opin. Colloid Interface Sci.* **2018**, *35*, 42.

[42] D. Hao, S. Xue-Zhao, S. Cheng-Min, H. Chao, X. Zhi-Chuan, L. Chen, T. Yuan, W. Deng-K, G. Hong-Jun, *Chin. Phys. B* **2010**, *19*, 106104.

[43] B. Manoj, A. G. Kunjomana, *IOP Conf. Ser.: Mater. Sci. Eng.* **2015**, *73*, 1.

[44] S. Mallik, S. S. Dash, K. M. Parida, B. K. Mohapatra, *J. Colloid Interface Sci.* **2006**, *300*, 237.

[45] A. Kausar, *AJPS* **2015**, *5*, 30.

[46] V. Khunova, J. Kristóf, I. Kelnar, J. Dybal, *EXPRESS Polym. Lett.* **2013**, *7*, 471.

[47] J. Hou, C. Cao, F. Idrees, X. Ma, *ACS Nano* **2015**, *9*, 2556.

[48] F. Yang, Z. Zhang, K. Du, X. Zhao, W. Chen, Y. Lai, J. Li, *Carbon* **2015**, *91*, 88.

[49] A. Esmaeili, M. H. Entezari, *J. Colloid Interface Sci.* **2014**, *432*, 19.

[50] Y. Liu, Q. Cai, H. Li, J. Zhang, *J. Appl. Polym. Sci.* **2012**, *128*, 517.

[51] M. Lamblin, L. Nassar-Hardy, J.-C. Hierso, E. Fouquet, F.-X. Felpin, *Adv. Synth. Catal.* **2010**, *352*, 33.

[52] S. Dehghani, S. Sadjadi, N. Bahri-Laleh, M. Nekoomanesh-Haghighi, A. Poater, *Appl. Organomet. Chem.* **2019**, *33*, e4891.

[53] M. Guo, H. Li, Y. Ren, X. Ren, Q. Yang, C. Li, *ACS Catal.* **2018**, *8*, 6476.

[54] S. Agrahari, S. Lande, V. Balachandran, G. Kalpana, R. Jasra, *J. Nanosci. Curr. Res.* **2017**, *2*, 2572.

[55] D. Samsonu, M. Brahmayya, B. Govindh, Y. Murthy, *S. Afr. J. Chem. Eng.* **2018**, *25*, 110.

[56] N. M. Patil, M. A. Bhosale, B. M. Bhanage, *RSC Adv.* **2015**, *5*, 86529.

[57] Y.-S. Feng, J.-J. Ma, Y.-M. Kang, H.-J. Xu, *Tetrahedron* **2014**, *70*, 6100.

[58] O. Verho, K. P. Gustafson, A. Nagendiran, C. W. Tai, J. E. Bäckvall, *ChemCatChem* **2014**, *6*, 3153.

[59] M. Nasrollahzadeh, S. M. Sajadi, A. Rostami-Vartooni, M. Alizadeh, M. Bagherzadeh, *J. Colloid Interface Sci.* **2016**, *466*, 360.

[60] S. Doherty, J. Knight, T. Backhouse, A. Bradford, F. Saunders, R. Bourne, T. Chamberlain, R. Stones, A. Clayton, K. Lovelock, *Cat. Sci. Technol.* **2018**, *8*, 1454.